

AJKFluids2015-14711

DIFFUSION CONTROL IN CIRCULAR JET USING COAXIAL TYPE DBD PLASMA ACTUATOR

Norimasa MIYAGI
Junior College of Nihon
University
Narashinodai 7-24-1,
Funabashi-city, Chiba, Japan

Hideo Ueki
Graduate school of Nihon
University
Kanda-surugadai 1-8-14,
Chiyoda-ku, Tokyo, Japan

Motoaki KIMURA
Nihon University
Kanda-surugadai 1-8-14,
Chiyoda-ku, Tokyo, Japan

ABSTRACT

This study investigated the use of a coaxial dielectric barrier discharge plasma actuator (DBD-PA) at a nozzle exit for jet diffusion control. In order to achieve enhanced mixing of the primary jet flow, the influence of the input voltage and frequency to the plasma actuator was examined. In the case of continuous operating, the secondary flow by the induced flow using coaxial plasma actuator is able to adjust the velocity gradient of the free shear layer near the jet nozzle. Intermittent control using the plasma actuator was also attempted by varying the intermittency frequency and the duty ratio. Based on the results of a PIV analysis, the optimum conditions for jet diffusion control were found to be an intermittency frequency that matched the preferred frequency and a duty ratio at 50%.

NOMENCLATURE

Re	Reynolds Number of main jet.
U_0	Main jet velocity.
d	Inner diameter of the nozzle and Plasma actuator exit.
ν	Kinetic viscosity.
f_n	Preferred frequency of single jet.
E	Applied voltage for Plasma actuator (PA) at AC.
f	Applied frequency for PA at AC.
f_d	Intermittency frequency of PA.
duty	Intermittent ratio.
T_b	Periodic time of PA driving.

INTRODUCTION

In recently year, the variously flow control device have been devised. One of the dynamic control method, there is a plasma actuator using DBD (Dielectric Barrier Discharge)⁽¹⁾⁻⁽³⁾. This is attractive what the response is earlier from the conventional mechanical control method, and weight is light, because it utilizes electromagnetic phenomenon. The authors, has continued research on the diffusion control in the early region (the potential core) of the circular jet, for the gas mixture

efficiently of the burner flames⁽⁴⁾⁽⁵⁾. The initial region of the circular jet, it corresponds to part of the initial mixing of the diffusion flame. Therefore, the diffusion control is intended to contribute to the promotion of the combustion. The diffusion control is intended to contribute significantly to the promotion combustion. There are two methods that diffusion control in the initial region. One is the adjustment of the free shear layer due to secondary flow.⁽⁴⁾ The other is the intermittent control of large-scale vortex rings which is a basic structure in the initial region of the jet.

In this study, it was applied the DBD plasma actuator that generates a plasma induced flow to the coaxial direction in the main jet. And, it aimed at diffusion control the potential core in the circular jet. First, it was confirmed the behavior of the jet due to the change applied parameters to the plasma actuator electrode, there are the applied voltage and the applied frequency. Secondary, it was attempted to intermittent operations of the plasma actuator, in order to control the large-scale vortex ring of jets. It was confirmed the effect in the case of changing the intermittency frequency and the intermittent ratio. To confirm the respective jet structure, it was experimented the visualization by the laser light sheet method, and it was analyzed by the PIV based on the visualization results.

EXPERIMENT

Coaxial DBD-PA and nozzle

Figure 1 shows a cross-sectional diagram of the coaxial type DBD-PA at the round nozzle exit, showing the main jet and the flow induced by the DBD-PA. The DBD-PA consists of an exposed electrode, an insulated electrode, and a dielectric layer. Plasma was generated by applying an alternating voltage of 2-6 kV at a frequency of 4-15 kHz. When a voltage is applied, an external body force (blowing force) is generated toward the insulated electrode from the exposed electrode⁽⁶⁾. Plasma

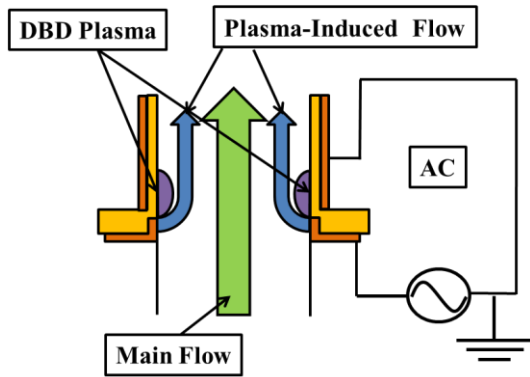


Fig.1 Schematic diagram of coaxial electrode actuator

induced flow affects the velocity distribution of the wall shear layer, and this effect is used to control the jet. Figure 2 shows the dielectric layer (Fig.2(a)), the covered and exposed electrode (Fig.2(b)-(c)), and their assembly (Fig.2(d)). The coaxial electrode was fabricated using a 1.0-mm-thick high-temperature polyimide molded body, and a 0.5-mm-thick copper pipe. The electrode is joined coaxially with an acrylic nozzle. The exposed and covered electrodes are placed coaxially in the nozzle wall. The height of the exposed electrode is 2 mm, and the height of the polyimide and the covered electrode is 10 mm. The acrylic nozzle was formed which has an inlet diameter of 25mm and an outlet diameter of 10 mm. An AC voltage is applied to the electrode, and flow is induced by the plasma. Diffusion control of the jet is thus attempted.

Experimental apparatus and conditions

Figure 3 and Table 1 show the experimental apparatus and experimental conditions used in the present study. Air was supplied to the nozzle from the compressor. The experiments velocity U_0 were conducted under Reynolds numbers (based on nozzle inner diameter) of 1,000 and 2,000. Seeding particles (Shell: Ondina oil #15) with diameters of approximately $1 \mu\text{m}$ were mixed with air for visualization of the jet. The jet cross section through its center was illuminated by a laser light sheet produced by an Nd:YAG laser (Omicron: LA-D40- CW, $\lambda = 532 \text{ nm}$), and images of the initial region of the jet up to $x/d = 6$, where x is the distance from the nozzle and d is the nozzle outlet diameter, were recorded using a high-speed camera (Photron: FASTCAMSA1.1) at 6,000 fps. The two-dimensional velocity distribution was determined by PIV analysis. To generate the plasma, a power source (PSI: PSI-PG1040F) was used to apply an AC voltage and frequency. At the continuous operation, the jet ejected at Reynolds number of 1000 ($U_0=1.55\text{m/s}$), and the electrodes were applied voltage of 2-6 kV with a frequency f of 4-15 kHz. At the intermittency operation, the jet ejected at Reynolds number of 2000 ($U_0=3.10\text{m/s}$), and the electrodes were applied voltage of 5kV with applied frequency of 15 kHz. The plasma actuator was operating with intermittency frequency f_d what is corresponding with preferred frequency f_n of the jet without PA

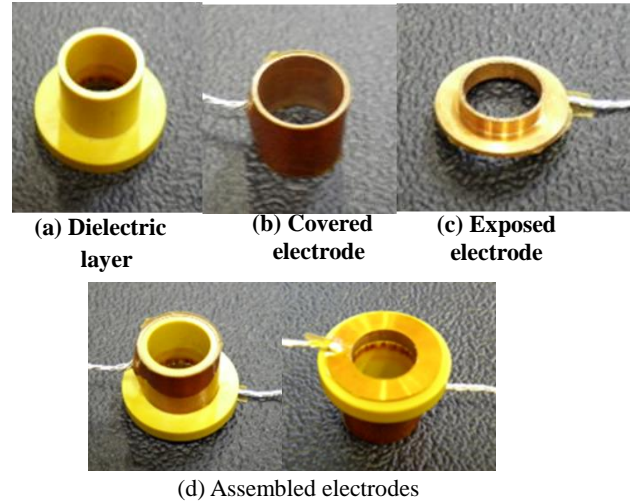


Fig. 2 Photographs of coaxial plasma actuator

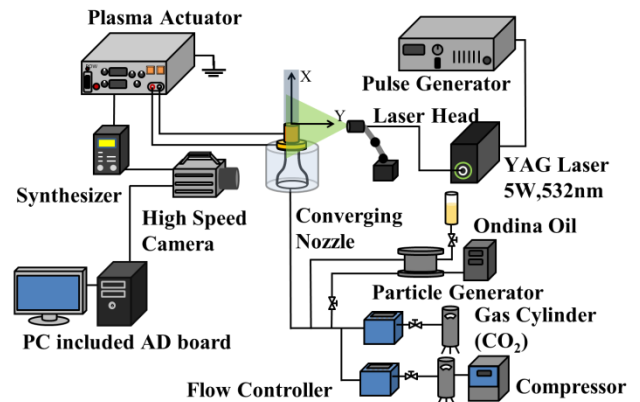


Fig. 3 Experimental setup

Table 1 Experimental conditions.

Continuous Operation	Main Jet	$Re = 1000 (U_0 = 1.55\text{m/s})$
	Inputted voltage	$E = 4.5\text{kV}, 5.0\text{kV}, 5.5\text{kV}$
	Inputted frequency	$f = 8\text{kHz}, 13\text{kHz}, 15\text{kHz}$
Intermittent Operation	Main Jet	$Re = 2000 (U_0 = 3.10\text{m/s})$
	Preffered frequency	$f_n = 160\text{Hz}$
	Inputted voltage	$E = 5.0\text{kV}$
	Inputted frequency	$f = 15\text{kHz}$
	Drive frequency (frequency ratio)	$f_d = 80\text{Hz} (f_d/f_n = 0.5)$ $f_d = 160\text{Hz} (f_d/f_n = 1.0)$ $f_d = 240\text{Hz} (f_d/f_n = 1.5)$ $f_d = 320\text{Hz} (f_d/f_n = 2.0)$ (duty = 10%)
	Intermittent ratio	duty = 10% ($T_b = 0.625\text{msec}$) duty = 50% ($T_b = 3.125\text{msec}$) duty = 90% ($T_b = 5.625\text{msec}$) ($f_d = 160\text{Hz}, T = 6.250 \text{ msec}$)

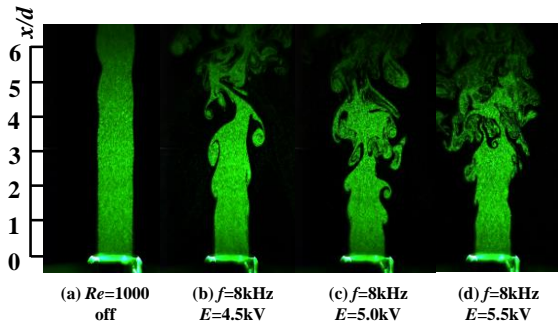


Fig. 4 Flow visualizations for different applied voltages

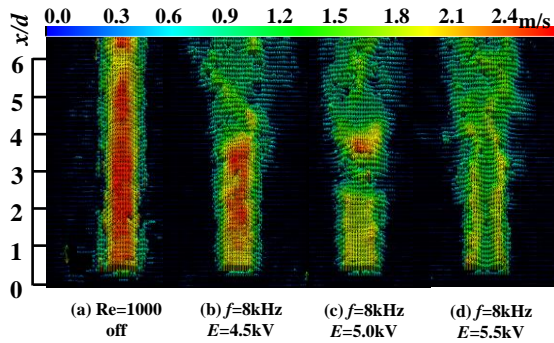


Fig.5 PIV analysis results for different applied voltages

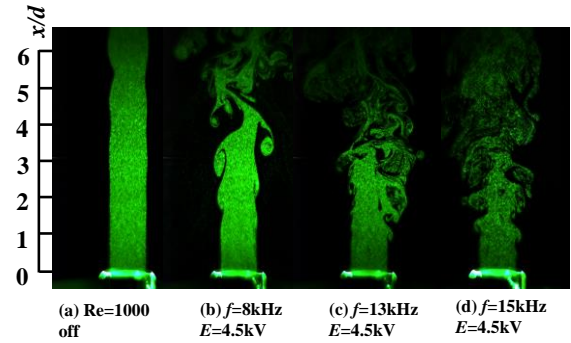


Fig. 6 Flow visualizations for different applied frequencies

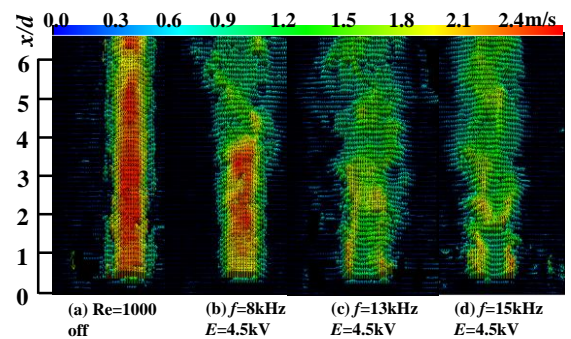


Fig. 7 PIV analysis results for different applied frequencies

operating. The intermittency duty cycle B/A , where A is the intermittent period and B is the PA operating period. The preferred frequency for $Re = 2,000$ and $d = 10$ mm is approximately 160 Hz. In order to increase the flow instability by amplifying the preferred frequency, intermittency frequencies of 80, 160, 240, and 320 Hz, and duty cycles of 10%, 50%, and 90% were used.

RESULT AND DISCUSSIONS

Jet control by continuous operating PA

Figure 4 shows visualizations of jet diffusion for continuous plasma-on and plasma-off conditions at Re of 1000. They are fixed the applied frequency of $f=8$ kHz, and are indicating at plasma-off (in fig(a)), as the applied voltage increasing (in fig(b)-(d)). Comparison of the plasma-on condition with the plasma-off, it reveals that the jet begins to collapse close to the outlet as a result of the plasma-induced flow. The jet begins to diffuse from about $x/d = 4$ at 4.5 kV, about $x/d = 3$ at 5.0 kV and 5.5 kV. As the applied voltage is increased, that is as the plasma induced flow increasing, the effect on the jet becomes more significant the occurrence of an instability of free shear layer. And it generates vortex rings. These vortex rings then collapse close to the nozzle. Figure 5 shows PIV results under the same conditions as in Fig. 4. The color bar indicates the velocity, at blue is slow and red is fast. Comparing with the plasma-on and off, it reveals that the potential core region, in which the velocity is not reduced by the

plasma induced flow, becomes shorter with increasing voltage. And the acceleration occurs in the free boundary layer near the plasma actuator wall with a corresponding deceleration near the jet center.

Figure 6 shows visualizations of jet diffusion for the continuous plasma-on and off conditions for various applied frequencies. The voltage is fixed at approximately 4.5 kV, and the applied frequency is varied as 8, 13, and 15 kHz. The jet diffuses from about $x/d = 4$ at 8 kHz, $x/d = 3$ at 13 kHz, and $x/d = 2.5$ at 15 kHz. Vortex rings are formed from about $x/d = 1$ at 13 and 15 kHz. Figure 7 shows a PIV result for the same applied frequencies as in Fig.6. In the plasma-off condition, the potential core extends to a distance of $x/d = 6$ or more. In the plasma-on condition, the jet begins to fluctuate from $x/d = 4$ at 8 kHz, and vortex rings are generated at $x/d = 1$. Moreover, the jet begins to diffuse from $x/d = 2.5$ at 15 kHz. Based on these results, the effect of the DBD-PA is small at 8 kHz for an applied voltage of approximately 4.6 kV, and as the frequency increases from 13 to 15 kHz, the velocity at the jet periphery is increased by the plasma induced flow. The strength of the induced flow increases with applied frequency, leading to an increased amount of disturbance to the jet. As the flow instability increases, vortex rings form earlier and they collapsed closer to the nozzle. Moreover, the jet diffusion starting position approaches the nozzle exit.

Figure 8 shows the cross-sectional velocity distribution at $x/d = 1$ to extract the PIV result in Fig.7. At the plasma-off condition, the center of the jet has a flat velocity profile. At 15

kHz and 13 kHz, the maximum velocity occurs at the jet periphery (at $y/d = \pm 0.4$), where y is the radial distance from the center of the jet center. In this region, the flow is accelerated by the flow induced by plasma generation. The velocity at the jet center is reduced because the ejection flow rate is constant. Furthermore, the cross-sectional area of the jet is increased by the flow instability.

Figure 9 shows a schematic diagram of the velocity distribution in the plasma actuator pipe. The flow in the plasma actuator is considered that the wall boundary layer becomes thicker by the skin friction of the pipe wall (Fig. (A)).

However, near-wall fluid is accelerated by the blowing forces by plasma discharge. And the velocity distribution is spouting such as in Fig(B). As the applied voltage and the applied frequency to the electrodes is increasing, the blowing force by plasma discharge acts strongly affect the free shear layer and the jet center velocity after the ejection.

Influence of intermittency on jet diffusion

In this section, we investigate the initial instability (K-H instability) of the jet at the nozzle exit, and the occurrence and collapse of vortex rings due to plasma-induced flow. The Reynolds number is 2000. Instability of the flow occurs at the nozzle exit, after which vortex rings are generated. Experimental findings indicate that the preferred frequency for this jet is approximately 160 Hz, where the Strouhal number, St , is 0.51 ($St = f_p d / U_0$; f_p : preferred frequency, d : nozzle outlet diameter, U_0 : issuing velocity)⁽⁷⁾. The intermittency frequency is a multiple of the preferred frequency. The applied frequency ($f=15$ kHz) and applied voltage ($E=4.8$ kV) were fixed. Also, in order to compare the continuous operation and intermittent operation, it was also performed the continuously operating under the same conditions. If the Reynolds number is 2000, the main velocity is faster than in the case of $Re=1000$, the acceleration region did not appear at the free boundary layer.

Figure 10 shows PIV results of the plasma-on and plasma-off conditions for various intermittency frequencies. The intermittency frequencies of 80, 160, 240, and 320 Hz, and a duty cycle of 10%. The red area indicates the potential core region, in which the initial velocity is maintained. Under the plasma-off condition, the potential core stretches to $x/d = 5$ from the nozzle exit. The length of the potential core also varies with the intermittency frequency. When the intermittency frequency is 160 Hz, which is the preferred frequency for the jet, the potential core length is the shortest ($x/d = 2-3$). At integral multiples of the preferred frequency, the intermittent plasma-induced flow amplifies the preferred frequency, thereby increasing the instability of the initial region. This increased instability promotes the generation of vortex rings in the vicinity of the outlet, which is the reason for the shortened potential core.

Figure 11 shows PIV result of jet diffusion for an intermittency frequency of 160 Hz and duty cycles of 10, 50, and 90, and under the plasma-off condition. The potential core of the jet is shortened by the generation of plasma. The

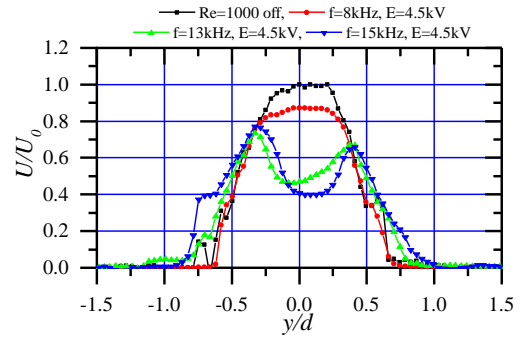


Fig. 8 Axial velocity distribution at $x/d=1$

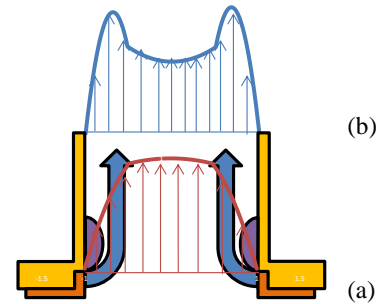


Fig. 9 Schematic diagram of velocity profile within plasma actuator

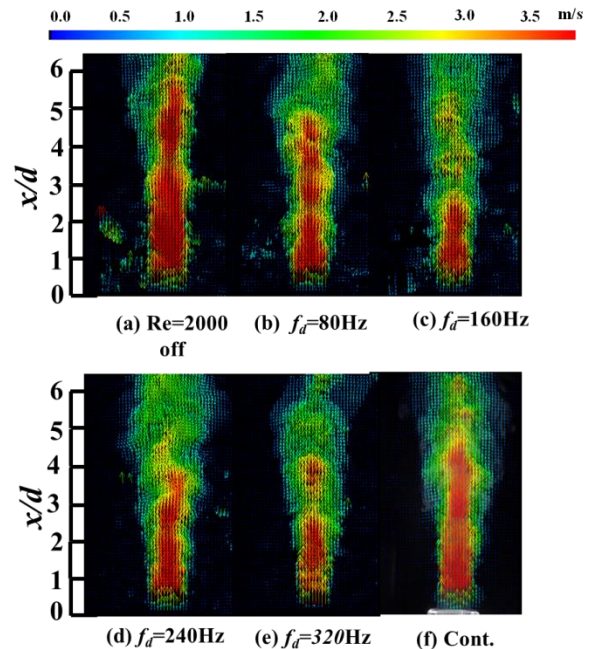


Fig. 10 PIV analysis results for intermittency frequencies

($E=4.8$ kV, $f=15$ kHz, duty ratio=10%)

potential core terminates at about $x/d = 4.5$ for a duty cycle of 90, $x/d = 1$ for a duty cycle of 50, and $x/d = 2.5$ for a duty cycle of 10. For a duty cycle of 50, the potential core length is the shortest. Although for a duty cycle of 10, the destabilizing

effect is reduced because the plasma generation time is short. For a duty cycle of 90, the plasma generation time is also short for generating vortex rings. The vortex pairs are generated in the vicinity of the nozzle exit. Since no large-scale vortex rings occur, the potential core is maintained. This indicates that there is an optimum duty cycle for increasing the instability of the jet near the nozzle exit, and this is close to 50.

Figure 12 shows the mean velocity profile at the jet center for various intermittency frequencies. Under the plasma-off condition, the potential core length is approximately $x/d = 4$. The velocity decreases rapidly at $x/d = 1.5$ for $f_d = 160$ Hz, and $x/d = 2.5$ for $f_d = 320$ Hz. As described above, the instability is increased when the intermittency frequency is an integer multiple of the preferred frequency. In addition, velocity decay that occurs for $f_d = 160$ Hz than for 320 Hz is thought to be because the former is the preferred frequency.

Figure 13 shows the mean velocity profile at the jet center for an intermittency frequency of 160 Hz and duty cycles of 10, 50, and 90. In the plasma-off condition, the nozzle exit velocity is maintained until $x/d = 4.5$. The velocity decreases from about $x/d = 3.5$ for a duty cycle of 90, $x/d = 1.5$ for a duty cycle of 50, and $x/d = 2$ for a duty cycle of 10. As described above, a duty cycle of 50 tends to promote jet instability, leading to the generation of vortex rings immediately outside the nozzle exit, and jet collapse also occurs close to the nozzle exit.

Figure 14 shows the velocity profiles at $x/d=1$, when was intermittent operation and continuous operation. The fig(a) shows in the case of the intermittency frequency change, and the fig(b) shows in the case of the intermittent ratio duty changing in each figure, the left side is the mean velocity, the right side is a turbulent intensity. In the case of $Re=2000$, the characteristic velocity profile that shown in fig.10 did not appear in continuous operation. Because the velocity of main jet is faster than the plasma induced flow. Also, compared with the case of plasma off condition, the velocity gradient is tight when it is continuously operation. In intermittent operation, for intermittency frequency of 160Hz and 320Hz, the mean velocity has reduced and turbulent intensity becomes stronger at the center of jet. It is considering that the instability of free shear layer has enhanced and the mixing of the jet reaches the jet center. In other frequency, the velocity fluctuation becomes stronger at periphery of the jet, it has not mixed until the jet center. For intermittent ratio 50, the fluctuation cycle of the induced flow by plasma generation is long, the velocity fluctuation occurs in the center of the jet, and the jet tends to diffuse. For intermittent ratio of 10 and 90, the fluctuation cycle is short, the velocity fluctuation occurs at periphery of the jet, it has not mixed until the jet center.

Based on these results, are summarized for the velocity fluctuation in intermittent operation. Figure 15 shows schematic diagram of the relationship between the plasma actuator driving time and the velocity distribution near the nozzle exit. Fig (a) shows for the case of duty = 10, fig(b) shows for the case of 50, and fig(c) shows for the case of 90. In the case of duty = 50%, it is able to provide a relatively large velocity fluctuations of the

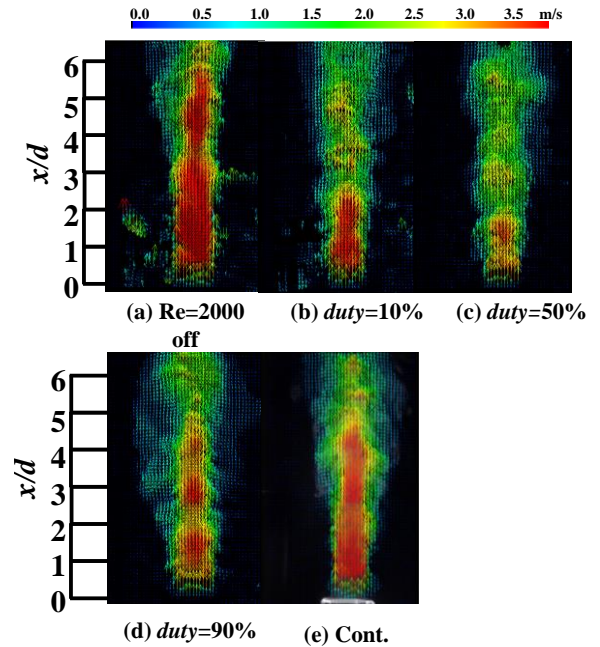


Fig. 11 PIV analysis results for different duty ratios ($E=4.8$ kV, $f=15$ kHz, $f_d=160$ Hz)

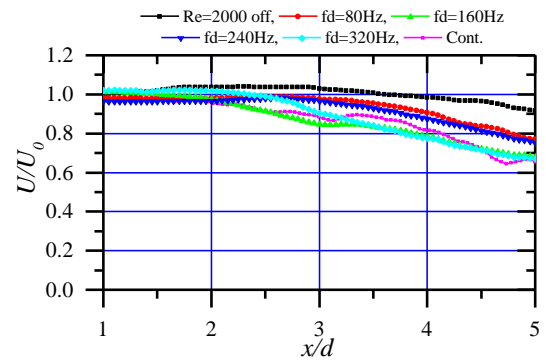


Fig. 12 Velocity along central axis ($E=4.8$ kV, $f=15$ kHz, duty ratio=10%)

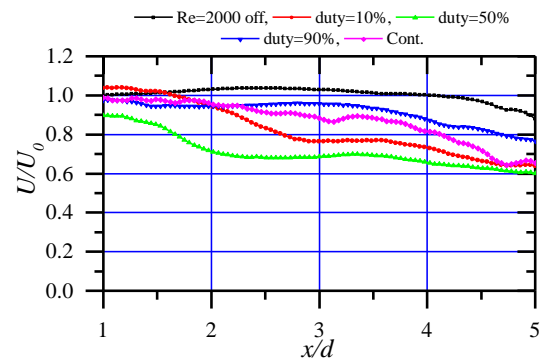


Fig. 13 Velocity along central axis ($E=4.8$ kV, $f=15$ kHz, $f_d=160$ Hz)

plasma induced flow by switching plasma-on and plasma-off. However, in the case of duty = 10%, the plasma actuator is short driving time in the driving cycle, and long time that the plasma is stopped, the velocity fluctuation due to the plasma actuator is relatively small at the time. In these intermittent ratios, it is possible to generate a periodic vortex ring by intermittent operation. Further, in the case of duty = 90%, because the driving time is long, it is close to the continuous operation. However, small velocity fluctuation occurs when the plasma actuator stopped. It is considering that a combination of secondary flow and intermittent fluctuations due to the induced flow.

SUMMARY

A coaxial DBD-PA has been applied to jet diffusion control. The plasma-induced flow was changed by varying the applied voltage, frequency, and intermittency. The velocity distribution could be controlled by the plasma-induced flow, and the following conclusions were reached.

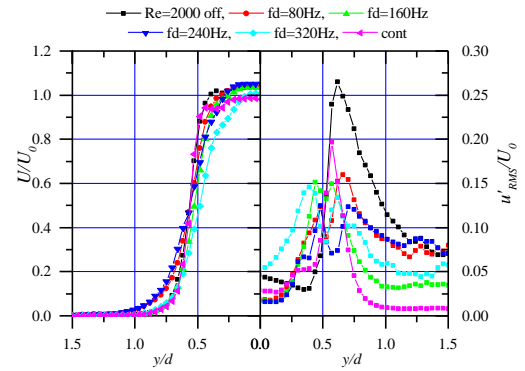
- 1) The diffusion effect increases as the applied voltage and frequency are increased.
- 2) Induced flow occurs near the surface of the inner wall of the nozzle, and the coaxial DBD-PA increases the velocity of the boundary layer.
- 3) The velocity distribution at the center of the jet cross section decreases with increasing velocity of the jet boundary layer due to the flow induced by the DBD-PA.
- 4) In the intermittent operation, for duty of 10 and 50, it is possible to provide a periodic fluctuation in conjunction with the intermittency frequency. And for duty of 90, it is able to provide a combined flow.
- 5) Intermittent ratio duty = 50% and intermittency frequency of 160Hz, it was possible to promote the diffusion of the jet.

ACKNOWLEDGMENTS

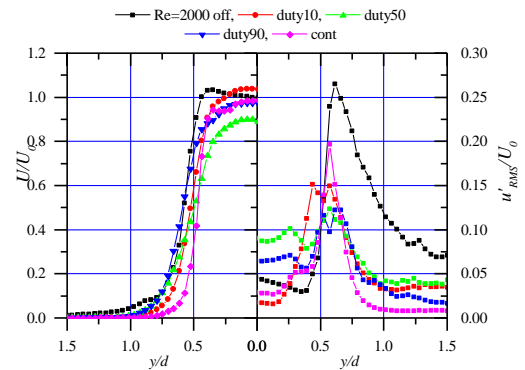
The present study was supported by Grants-in-Aid for Scientific Research (C) (KAKENHI Nos. 22560176 and 25420132).

REFERENCES

- (1) Fukagata, K., Yamada, S., and Ishikawa, H., "Plasma Actuators Fundamentals and Research Trends", *Journal of Japan Society of Fluid Mechanics*, Vol. 29, No. 4 (2010), pp. 243–250 (in Japanese).
- (2) Corke, T. C., Enloe, C. L. and Wilkinson, S. P., "Dielectric barrier discharge plasma actuators for flow control", *Annual Review of Fluid Mechanics*, Vol.42 (2010), pp.505-529.
- (3) Moreau, E., "Airflow Control by no-thermal plasma actuators", *Journal of Physics D: Applied Physics*, 40, No.3 (2007), pp.605-636.
- (4) Miyagi, N., Hodoya, K., Fujita, H., Shoji, H., Kimura, M., "Study of Active Jet Control by Acoustically Driven Secondary Film Flow Influence of Velocity Ratio and Acoustic Strouhal Number" *JSME International Journal B*, Vol.49, No.4, (2006), pp. 974-979.

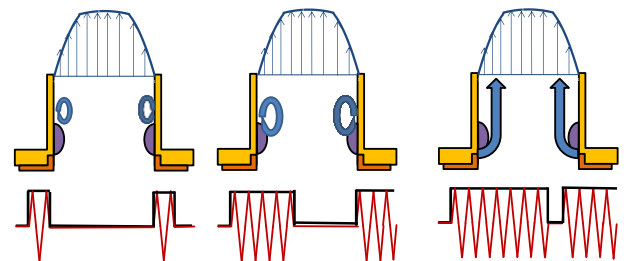


(a) for different intermittency frequencies



(b) for different duty ratios

Fig. 14 Axial velocity distributions at $x/d=1$ ($E=4.8$ kV, $f=15$ kHz)



(a) duty=10% (b) duty=50% (c) duty=90%

Fig. 15 Schematic diagram of velocity variations within plasma actuator for different duty ratios

- (5) Kawai, Y., Kimura, M., "Relationship between Preferred Frequency and Diffusion by Jet Density and Exit Velocity Distributions", *JSME journal B*, Vol.77, No.775 (2011), pp.106-114
- (6) Enloe, C. L., McLaughlin, T. E., VanDyken, R. D., Kachner, K. D., Jumper, E. J., et al., "Mechanisms and responses of a single-dielectric barrier plasma actuator" *AIAA Journal*, Vol. 42, No. 3 (2004), pp. 595-604.
- (7) Petersen, R. A. and Samet, M. M., "On the preferred mode of jet instability", *J. Fluid Mech.* 194, (1988), pp. 153-157.